

# Etch Rates for Micromachining Processing

Kirt R. Williams, *Student Member, IEEE*, and Richard S. Muller, *Life Fellow, IEEE*

**Abstract**—The etch rates for 317 combinations of 16 materials (single-crystal silicon, doped, and undoped polysilicon, several types of silicon dioxide, stoichiometric and silicon-rich silicon nitride, aluminum, tungsten, titanium, Ti/W alloy, and two brands of positive photoresist) used in the fabrication of microelectromechanical systems and integrated circuits in 28 wet, plasma, and plasmaless-gas-phase etches (several HF solutions,  $\text{H}_3\text{PO}_4$ ,  $\text{HNO}_3 + \text{H}_2\text{O} + \text{NH}_4\text{F}$ , KOH, Type A aluminum etchant,  $\text{H}_2\text{O} + \text{H}_2\text{O}_2 + \text{HF}$ ,  $\text{H}_2\text{O}_2$ , piranha, acetone, HF vapor,  $\text{XeF}_2$ , and various combinations of  $\text{SF}_6$ ,  $\text{CF}_4$ ,  $\text{CHF}_3$ ,  $\text{Cl}_2$ ,  $\text{O}_2$ ,  $\text{N}_2$ , and He in plasmas) were measured and are tabulated. Etch preparation, use, and chemical reactions (from the technical literature) are given. Sample preparation and MEMS applications are described for the materials. [193]

## I. INTRODUCTION

WHEN DESIGNING a new process to fabricate micro-machined devices, the etch rate of each layer that is to be patterned must be known. While the etch rates of many etchants that target specific materials (e.g., thermally grown silicon dioxide in 5:1 buffered hydrofluoric acid) are commonly known, the etch rates of the masking and underlying films are frequently not quoted in the literature. This paper provides this information for 317 different combinations of 16 materials and 28 etches used in the micromachining of microelectromechanical systems (MEMS) and in integrated-circuit processing. These etch-rate data, based on tests performed in the U. C. Berkeley Microfabrication Laboratory (Berkeley Microlab), are tabulated in Tables I and II.

The first sections of this paper describe the preparation and use of the wet and dry etches in Tables I and II, listing chemical reactions and variation of etch rate with such factors as temperature and concentration, based on literature on the subject. Recognizing that there are many sources of etch-rate variation, brief lists of these sources are given at the end of these wet- and dry-etch sections. The succeeding sections describe the sample preparation and MEMS applications for each of the materials, the measurement techniques used, and finally discuss the data in the tables.

## II. THE WET ETCHES

### A. Comparison of Wet and Dry Etches

The etches in the tables are divided into wet and plasma and plasmaless-gas-phase (“dry”) etches. The advantages and disadvantages of wet and dry etching are well known [1],

Manuscript received January 10, 1996; revised July 1, 1996. Subject Editor, K. Najafi. This work was supported by the Berkeley Sensor & Actuator Center. The authors are with the Berkeley Sensor & Actuator Center, University of California at Berkeley, Berkeley, CA 94720-1770 USA.

Publisher Item Identifier S 1057-7157(96)08843-9.

[2]; the most important for micromachining are as follows. Wet etching is usually isotropic (desirable in some cases), can have a selectivity that depends on crystallographic direction, and can be very selective over masking and underlying layers. Plasma etching uses fresh chemicals for each etch (resulting in less chemical-related etch-rate variability) and can be vertically anisotropic (as well as isotropic), allowing the patterning of narrow lines. When removing a sacrificial layer in micromachining, wet etching has the disadvantage of capillary-force pull-down of free-standing structures [3]. This can be avoided by using a supercritical-liquid drying process [4] or by switching to a dry-etched sacrificial layer [5], [6].

### B. Wet-Etch Chemicals

All of the chemical mixtures made in the Berkeley Microlab and discussed in the next section are by volume, with one noted exception. Conversely, those prepared and bottled by chemical-supply companies are by weight.

Many of the chemicals used in wet etching are not supplied in pure form. Acetic acid is supplied pure and sulfuric acid nearly pure (96%), while other acids normally come in lower concentrations for various reasons. Phosphoric acid is a deliquescent solid at room temperature [7]. Above the 85% concentration at which it is supplied, it is very viscous and tends to oligomerize into polyphosphoric acids. Pure hydrofluoric acid has a boiling point of  $19.5^\circ\text{C}$  [7]. As supplied at 49% concentration, it has a greatly reduced vapor pressure, increasing personal safety and allowing room-temperature storage in unpressurized containers. Nitric acid is a liquid in the range near room temperature, but tends to decompose above the supplied concentration of 70%. Sulfuric [8] and acetic [9] acids are liquids that are completely miscible in water at room temperature at all concentrations to 100%. Hydrofluoric acid [10] is also a completely soluble liquid below its boiling point.

An extensive list of other wet etchants for a variety of semiconductors, metals, insulators, and other compounds has been compiled by Vossen and Kern [11].

### C. Information about Individual Wet Etches

In this section, each etchant is listed by its name from Table I in italics, followed by its complete name, target material, notes on use, information on the reaction(s) that occur, if known from the technical literature, and major sources of etch-rate variation. For brevity, etchants with the same reactions (e.g., all HF solutions) are discussed together. The etchants are grouped by target material. Unless otherwise noted, all of the wet etchants are isotropic.

TABLE I

**Wet-Etch Rates for Micromachining and IC Processing (Å/min)**

The top etch rate was measured by the authors with fresh solutions, etc. The center and bottom values are the low and high etch rates observed by the authors and others in our lab under less carefully controlled conditions.

ETCHANT EQUIPMENT CONDITIONS	TARGET MATERIAL	MATERIAL															
		SC Si <100>	Poly n*	Poly undop	Wet Ox	Dry Ox	LTO undop	PSG unant	PSG annal	Stoic Nitrid	Low-σ Nitrid	Al/2% Si	Sput Tung	Sput Ti	Sput Ti/W	OCG \$20PR	Olin HnPFR
Concentrated HF (49%) Wet Sink Room Temperature	Silicon oxides	-	0	-	23k 18k 23k	F	>14k	F	36k	140	52	42	<50	F	-	P 0	P 0
10:1 HF Wet Sink Room Temperature	Silicon oxides	-	7	0	230	230	340	15k	4700	11	3	2500	0	11k	<70	0	0
25:1 HF Wet Sink Room Temperature	Silicon oxides	-	0	0	97	95	150	W	1500	6	1	W	0	-	-	0	0
5:1 BHF Wet Sink Room Temperature	Silicon oxides	-	9	2	1000 900 1080	1000	1200	6800	4400 3500 4400	9 3 4	4	1400	<20 0.25 20	F	1000	0	0
Phosphoric Acid (85%) Heated Bath with Reflux 160°C	Silicon nitrides	-	7	-	0.7	0.8	<1	37	24 9 24	28 19 42	19 19 42	9800	-	-	-	550	390
Silicon Etchant (126 HNO <sub>3</sub> : 60 H <sub>2</sub> O : 5 NH <sub>4</sub> F) Wet Sink Room Temperature	Silicon	1500	3100 1200 6000	1000	87	W	110	4000	1700	2	3	4000	130	3000	-	0	0
KOH (1 KOH : 2 H <sub>2</sub> O by weight) Heated Stirred Bath 80°C	<100> Silicon	14k	>10k	F	77 41 77	-	94	W	380	0	0	F	0	-	-	F	F
Aluminum Etchant Type A (16 H <sub>3</sub> PO <sub>4</sub> : 1 HNO <sub>3</sub> : 1 HAc : 2 H <sub>2</sub> O) Heated Bath 50°C	Aluminum	-	<10	<9	0	0	0	-	<10	0	2	6600	-	0	-	0	0
Titanium Etchant (20 H <sub>2</sub> O : 1 H <sub>2</sub> O <sub>2</sub> : 1 HF) Wet Sink Room Temperature	Titanium	-	12	-	120	W	W	W	2100	8	4	W	0	8800	-	0	0
H <sub>2</sub> O <sub>2</sub> (30%) Wet Sink Room Temperature	Tungsten	-	0	0	0	0	0	0	0	0	0	<20	190 190 1000	0 0 150	60 60 150	<2	0
Piranha (-50 H <sub>2</sub> SO <sub>4</sub> : 1 H <sub>2</sub> O <sub>2</sub> ) Heated Bath 120°C	Cleaning off metals and organics	-	0	0	0	0	0	-	0	0	0	1800	-	2400	-	F	F
Acetone Wet Sink Room Temperature	Photoresist	-	0	0	0	0	0	-	0	0	0	0	-	0	-	>4k	>59k

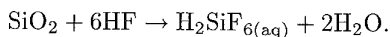
Notation: - = test not performed, but known to work (≥ 100 Å/min); W = not performed, but known to be Fast (≥ 10 kÅ/min); P = some of film Peeled during etch or when rinsed; A = film was visibly Attacked and roughened. Etch areas are all of a 4-inch wafer for the transparent films and half of the wafer for single-crystal silicon and the metals. Etch rates will vary with temperature and prior use of solution, area of exposure of film, other materials present (e.g., photoresist), film impurities and microstructure, etc. Some variation should be expected.

All wet etching was done at room temperature (about 20°C in the temperature-controlled Berkeley Microlab), unless otherwise indicated. All wet etching was done with fresh solutions, agitating occasionally. To remove the vapors created by the etchants, all wet etching was done under fume hoods.

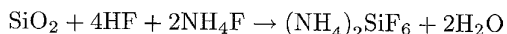
1) *Silicon Dioxide Wet Etchants*: Notes: All of the silicon dioxide etchants given here are based on hydrofluoric acid. HF-based etchants are used mainly for etching silicon dioxide, although they can also be used to remove silicon nitride. In our tests, they were observed to etch polysilicon very slowly, but other researchers have noted that various solutions attack polysilicon at the grain boundaries, resulting in noticeable surface roughness [12], [13]. Recent research indicates that HF can diffuse through thin (<0.2- $\mu\text{m}$ ) polysilicon to etch underlying low-temperature oxide (LTO) [13], [14].

HF-based solutions should be handled with polypropylene, high-density polyethylene (HDPE), polytetrafluoroethylene (PTFE), polyvinylidene fluoride (PVDF), or similar-material containers and tools (not glass containers, which will be attacked). In the Berkeley Microlab, molded PVDF has replaced welded polypropylene in most room-temperature chemical tanks in an effort to reduce particle counts and contamination from chemicals that have leaked into cracks in the welds. PTFE cassettes are used.

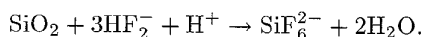
Reaction: Several similar reactions for the HF-based etching of silicon dioxide are given in the literature. For pure HF etching, the overall reaction is [2], [15]



Kikuyama *et al.* [16] give the reaction in BHF solutions as



and the reaction involving the  $\text{HF}_2^-$  ion (discussed below) as



HF is a weak acid; except when present in very small concentrations, it does not completely dissociate into  $\text{H}^+$  and  $\text{F}^-$  ions in water [16]. Judge [17] and Deckert [18] have found the etch rate of both silicon dioxide and silicon nitride to increase linearly with the concentrations of both HF and  $\text{HF}_2^-$  for concentrations lower than 10 M, while being independent of the concentration of  $\text{F}^-$  ions alone. The  $\text{HF}_2^-$  complex attacks oxide about 4.5 times faster than HF. Higher-order complexes, such as  $\text{H}_2\text{F}_3^-$ , appear to occur at higher HF concentrations (e.g., in 49% HF) and attack oxide even faster than  $\text{HF}_2^-$  [17]. Thus, the etch rate increases faster than linearly with HF concentration.

In buffered 15 M HF solutions, for pH values above about 1, the concentration of  $\text{HF}_2^-$  is greater than that of HF [17]. For more acidic solutions, there is sufficient hydrogen to combine with the fluoride to make HF the dominant species. As HF and  $\text{HF}_2^-$  are consumed, the etch rate decreases. Buffering with  $\text{NH}_4\text{F}$  helps keep the pH and thus the concentrations of HF and  $\text{HF}_2^-$  constant, stabilizing the etch rate [16].

The etch rate of silicon dioxide increases with temperature. Judge gives an apparent activation energy of 0.29 eV over the temperature range 30 to 60 °C for concentrated HF and higher activation energies as the ratio of  $\text{NH}_4\text{F}$  to HF increases [17].

By contrast, Parisi *et al.* found the apparent activation energy to be independent of buffer ratio at 0.43 eV over the range 25 to 55°C [19].

Tenny and Ghezzi found the etch rates of annealed phosphorus-doped LTO to increase monotonically with both  $\text{P}_2\text{O}_5$  content and concentration of HF in BHF solutions [20], the same result found by Monk for HF solutions [13]. Tenny and Ghezzi concluded that the  $\text{P}_2\text{O}_5$  in the glass etches more rapidly than the  $\text{SiO}_2$ . They also found that for annealed borosilicate glasses, the etch rate in strong solutions of HF decreases for small concentrations of  $\text{B}_2\text{O}_3$ , before rising for concentrations above 17 molar percent.

Monk [13] has done a thorough characterization on the transport of HF and  $\text{H}_2\text{SiF}_6$  during the undercutting of oxide sacrificial layers. He found that for deep micromachined undercuts, the etch rate is controlled by diffusion (i.e., slower for longer undercutting) and is not affected by agitation of the bath.

*Concentrated HF (49%)*: Concentrated hydrofluoric acid (49% by weight, remainder water). Produced commercially.

Notes: Etches oxides very rapidly. Often used to remove sacrificial oxide when micromachining. Concentrated HF tends to peel off photoresist, while lower concentrations (less than 3:1) do not [21].

*10:1 HF*: 10:1 HF:H<sub>2</sub>O: concentrated HF (49% HF).

Notes: Typically used for stripping oxide and for HF dips, diluted HF is cheaper than buffered HF.

*25:1 HF*: 25:1 HF:H<sub>2</sub>O: concentrated HF (49% HF).

Notes: This slow etch is used for HF dips to strip native oxide without removing much of the other oxides that may be on a wafer.

*5:1 BHF*: 5:1 buffered hydrofluoric acid (also known as buffered oxide etch, or BOE). "5:1" refers to five parts by weight of 40-weight-percent ammonium fluoride (the buffer) to one part by weight 49-weight-percent hydrofluoric acid, which results in a total of about 33%  $\text{NH}_4\text{F}$  and 8.3% HF by weight [22]. Produced commercially, the pH is about 3.

Notes: This etchant can be masked with photoresist (the adhesion is much better than in concentrated HF). Because it is buffered, its etch rate does not vary as much with use. It is the often best choice for controlled etching of oxides. Some researchers have, however, observed a slight attack of 5:1 BHF on polysilicon, causing surface roughening [12].

2) *Silicon Nitride Wet Etchant*:

*Phosphoric acid (85%)*: Phosphoric acid (85% by weight, remainder water) at 160°C. Produced commercially. In the Berkeley Microlab, this etchant is heated in a PFA tank with a Pyrex reflux system to return condensed water vapor to the solution.

Notes: Phosphoric acid is used for the wet etching of silicon nitride. Our nitride is typically masked with densified PSG (densifying at 1000°C for an hour does not affect low-stress nitride). If the PSG mask is not densified it is removed faster and may also have pores through which the acid can seep. The nitride can also be patterned with polysilicon.

At 160 °C, the vapor pressure over 85% phosphoric acid is slightly more than one atmosphere, with the vapor being virtually pure water [23].

Reaction: The literature does not list a chemical reaction for the etching of silicon nitride. Gelder and Hauser propose that the water in the solution hydrolyzes the nitride to some form of hydrous silica and ammonia [23].

Gelder and Hauser [23] report the "real" activation energy for the etching of silicon nitride in a constant concentration of 94.5% phosphoric acid as 0.99 eV. The "apparent" activation energies, taken with the etch temperature and boiling point being the same (i.e., for varying concentrations of  $\text{H}_3\text{PO}_4$ ) are 0.55 eV for silicon nitride, 1.20 eV for silicon dioxide, and 1.15 eV for silicon. These apparent activation energies take into account the effects of temperature on both concentration of  $\text{H}_3\text{PO}_4$  in the solution and the etch reactions themselves.

As the water content in the etch bath decreases (e.g., due to evaporation), the etch rate of silicon nitride decreases, while the etch rate of silicon dioxide increases [23], so the use of a reflux system is important in maintaining a constant etch rate and mask selectivity.

### 3) Isotropic Silicon Wet Etchant:

*Silicon etchant:* Wet silicon etchant. This solution is mixed and bottled in the Berkeley Microlab from 126:60:5  $\text{HNO}_3$  (70%) :  $\text{H}_2\text{O}$  :  $\text{NH}_4\text{F}$  (40%).

Notes: This etch, similar to the  $\text{HNO}_3 + \text{H}_2\text{O} + \text{HF}$  etches discussed in a series of papers by Robbins and Schwartz [2], [24], is used mainly for polysilicon wet etching. The slight change in chemistry was used earlier at Trilog [25]. It can be masked by photoresist.

Reaction: A simplified description of the reaction is that the nitric acid in the solution oxidizes the silicon, then the hydrofluoric acid (formed from the fluoride ions in this acidic solution) etches the oxidized compound. Many metal etches not discussed in this paper also remove material in this two-step manner. The overall reaction is [2], [26]



Turner has found the peak etch rate of silicon to occur at an  $\text{HF}:\text{HNO}_3$  ratio of 4.5, the same ratio as in the balanced reaction given above [26]. The rate-limiting step for the etch solution in this table, which has a low HF concentration, is the supply of HF to the reaction site [26]. The etch rate of a given bath decreases with use as the HF is depleted. The use of  $\text{NH}_4\text{F}$  rather than HF results in a buffer action, keeping the HF and  $\text{HF}_2^-$  (both responsible for etching the oxidized silicon) concentrations from changing as rapidly with use [25]. Used solutions turn yellow due to dissolved NO gas.

### 4) Orientation-Dependent Silicon Wet Etchants:

*KOH 80 °C:* Potassium hydroxide solution at 80 °C. Mixed from 1 kg KOH pellets : 2 liters  $\text{H}_2\text{O}$ . This solution is about 29% KOH by weight because the KOH pellets normally contain 10 to 15% water [27]. It is heated in a perfluoroalkoxy polytetrafluoroethylene (PFA) tank with recirculating pump.

Notes: This solution is self heating. It should be allowed to equilibrate before using for a controlled temperature. When etching single-crystal silicon, the silicon can be masked with silicon nitride. To reduce undercutting of the nitride mask, a HF dip should be carried out immediately before the nitride deposition to remove any native oxide.

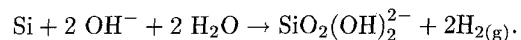
We have found that the KOH in unagitated solutions tends to stratify, resulting in etch-rate variation from the top to the bottom of the solution. This problem was solved by the use of a recirculation pump.

KOH is used for orientation-dependent etching (ODE) of single-crystal silicon. ODE's attack {111}-type planes, which have a high bond density, much more slowly than other planes [2], [28]. (Unfortunately, this high-bond-density reasoning for slow-etch-rate planes cannot be extended to explain the etch-rate ratio between {100} and {110} planes [28].) The etch rate listed in Table I is the one perpendicular to the surface of the (100) wafers used for this etch-rate test. KOH stops etching on very heavily doped p-type material [29].

Isopropyl alcohol is sometimes added to KOH solutions. This decreases the etch rate, but improves uniformity, reducing the requirement for stirring [30]. It also slows {110}-plane and accelerates {111}-plane etching (not affecting {100} planes much) and lessens the severity of the etching of convex corners [28].

(Other inorganic hydroxides [29], [30], organic hydroxides such as tetramethyl ammonium hydroxide (TMAH) [31], [33], and ethylenediamine pyrocatechol (EDP) [29], [30], an organic base, are orientation-dependent etchants similar to KOH. In the Berkeley Microlab and others, EDP has been found to be better than KOH at stopping abruptly at heavily boron-doped regions [29], [32]. TMAH has the advantages of not being a source of sodium (which contaminates the gate oxide in MOS circuitry) and not attacking aluminum when it has been "doped" with a small amount of silicon [33].)

Reaction: Several different reactions for KOH etching of silicon are listed in the literature [2], [30]. Seidel *et al.* list the gross reaction as [30]



Glembocki *et al.* list a very similar reaction [34]. This chemical reaction is independent of the source of the hydroxide ion, whether LiOH, NaOH, or KOH, in agreement with experiment.

The dependence of the reaction on p-type doping is explained by Seidel *et al.* [30] and also by Raley *et al.* [32]: At intermediate steps in the etch, four free electrons are generated that reside near the surface before being exchanged. P-type doping reduces this surface supply of electrons. The etch rate decreases as the fourth power of the concentration for p-type doping beyond degeneracy, which occurs at about  $2 \times 10^{19} \text{ cm}^{-3}$  active boron atoms.

Seidel found the etch-rate ratio for {110} to {100} to {111} planes to be about 160:100:1 at 20 °C, decreasing to 50:30:1 at 100 °C [30]. In contrast, Kendall measured even higher ratios of 400:200:1 at 85 °C and discussed the extreme difficulty in making these measurements [28].

The etch rate in KOH increases with temperature. Seidel *et al.* give activation energies for the concentration of KOH in Table I (29% by weight) of 0.59 eV for (100) silicon and 0.84 eV for silicon dioxide [30]. They also found that, at 80 °C, the etch rates of (100) silicon and silicon dioxide peak at concentrations of about 18 and 34 weight %, respectively. Lower concentrations of either  $\text{H}_2\text{O}$  or  $\text{OH}^-$ , both used in the reaction, result in lower etch rates. The surfaces, however,

appear rough and insoluble white residues form for KOH concentrations below 20% [35]. The temperature and KOH concentration effects on the etch rate ( $ER$ ) of (100) silicon were empirically found to fit well to the equation [30]

$$ER_{\text{Si in KOH}} = k_0[\text{H}_2\text{O}]^4[\text{KOH}]^{1.4}e^{-E_A/kT}$$

where the etch rate is in  $\mu\text{m/h}$ , the concentrations are in mol/liter,  $k_0 = 2480 \mu\text{m/hr} \cdot (\text{mol/liter})^{-4.25}$ , and  $E_A = 0.595 \text{ eV}$ .

#### 5) Metal Wet Etchants:

**Aluminum Etchant Type A:** Aluminum etchant Type A at 50 °C. This solution, sold commercially, is composed of 80% phosphoric acid, 5% nitric acid, 5% acetic acid, and 10% water [36]. Some formulations may include a surfactant. According to the manufacturer, this etchant is designed to etch aluminum at 6000 Å/min at 50 °C. It is heated in a PFA tank.

Notes: This etch is used for wet etching of aluminum. It can be masked with photoresist.

Reaction: In this multistep etch [37], the aluminum is first oxidized by the nitric acid. The phosphoric acid and water simultaneously etch the resulting oxide. With the concentrations given, these two processes occur at roughly the same rate, so that either could be the rate-limiting step [37]. Because the phosphoric acid also removes the native aluminum oxide, no additional component is needed for this purpose.

The etch rate increases with temperature and decreases significantly with use due to depletion of the active chemicals.

Similar solutions with a reduced fraction of water etch more rapidly [37]. Agitating aids etch-rate uniformity across a wafer, as well as helping to remove the hydrogen bubbles that evolve. If not removed, these bubbles can block the flow of reactant to the surface, resulting in localized etch nonuniformity.

**Titanium Etchant:** Mixed from 20:1:1  $\text{H}_2\text{O} : \text{HF} (49\%) : \text{H}_2\text{O}_2 (30\%)$ .

Notes: HF is the active ingredient in this etchant, so it also etches oxides. Raising the fraction of HF in the solution increases the etch rate. Titanium etched in this solution can be masked with photoresist.

Reaction: No reaction is given in the literature. Titanium is known to be readily oxidized, so it likely forms an oxide from the water and peroxide, which is readily etched by the HF in this solution.

**$\text{H}_2\text{O}_2 (30\%)$ :** Hydrogen peroxide (30% by weight). Produced commercially.

Notes: This etchant is used to wet-etch tungsten and its alloys, which can be masked with photoresist. We have observed that  $\text{H}_2\text{O}_2$ -etching of tungsten sometimes leaves a residue.

Reaction: In this etch, a film of tungsten oxide is formed that is dissolved in the hydrogen peroxide [38]. This etchant also etches tungsten/titanium alloys, but not pure titanium.

The etch rate rises with temperature, but any significant increase may cause a photoresist mask to be eroded or to peel. CVD silicon-based masking layers, successful for other films, cannot be used with tungsten, as the silicon reacts to form tungsten silicides during the high-temperature deposition. Sputtered aluminum is a suitable mask layer, although when used, it becomes difficult to observe the end of the aluminum etch either optically or electrically.

(Another tungsten etch, which has been found in our lab not to leave the residue mentioned above, contains 1 liter  $\text{H}_2\text{O}$ , 34 g  $\text{K}_3\text{Fe}(\text{CN})_6$ , 13.4 g KOH, and 33 g  $\text{KH}_2\text{PO}_4$ . It can be patterned with photoresist, does not attack oxide or nitride at an appreciable rate, and etches tungsten at 340 Å/min).

#### 6) Wet Wafer Cleaning:

**Piranha 120 °C:** Piranha in 120 °C heated bath. In the Berkeley Microlab, piranha consists of about 5.6 liters of 96%  $\text{H}_2\text{SO}_4$  heated to 120 °C in a PFA tank, to which 100 ml of 30%  $\text{H}_2\text{O}_2$  is added immediately before each use.

Notes: Piranha has been in use for wafer cleaning for decades [1], [39], [40]. The term refers to a hot solution of  $\text{H}_2\text{SO}_4$  and  $\text{H}_2\text{O}_2$  mixed in any ratio [39], [40]. In lower ratios of  $\text{H}_2\text{SO}_4$  to  $\text{H}_2\text{O}_2$  (e.g., 5:1), the solution is noticeably self-heating (no external heat source is needed).

Piranha is used in the Berkeley Microlab for 10 min to clean organic and metallic contaminants from wafers before furnace steps. Kern and Puotinen [41] have observed that the desorption of 90% of monatomic metal films from silicon into similar acidic peroxide solutions can take several minutes.

Reaction: Like other acidic hydrogen peroxide solutions, piranha strips photoresist and other organics by oxidizing them, and removes metals by forming complexes that stay in the solution [41], [42]. It does not affect silicon dioxide and silicon nitride and has the minor effect on bare silicon of forming a thin layer of hydrous silicon oxide [41]. This oxide film is typically removed with a short (10-s) 10:1 or 25:1 HF dip after the piranha clean and rinse.

**Acetone:** Acetone spray from a photoresist developing machine.

Notes: Acetone is used to strip photoresist (PR) and for lift-off patterning of films [1], [2]. The machine used in the Berkeley Microlab gives a stream of fresh acetone for PR stripping.

An acetone bath would be used for liftoff processes [1], [2]. Lift-off processes can be sped up by heating the acetone (with a loose lid to slow evaporative loss) or by placing it in an ultrasonic tank.

While acetone readily stripped the photoresists listed in this table, its effectiveness depends on the processing the PR has gone through. Heating the PR by a few tens of degrees above 120 °C, either while hardbaking or during a process step, will make it significantly harder to dissolve [1]. Some plasma processing gives rise to a similar effect (known as "plasma hardening"). In such cases, an oxygen plasma, a commercial PR stripper (such as Baker PRS-2000), or piranha can usually be used to remove the PR.

Reaction: Acetone breaks down the structure of the photoresist, making it soluble [1].

#### D. Wet-Etch-Rate Variation

The wet-etch rates given in Table I can vary for reasons that are usefully divided into three groups: the etch setup, the material being etched, and the layout and structure on the substrate. The most significant effects on the wet-etch rate in each of these categories are as follows (due to space constraints, the reader is referred to the references for detailed information on these sources of etch-rate variation).

Etch-rate variation due to the etch setup is a function of 1) temperature [43]; 2) loss of reactive species [43]; 3) loss of liquids to evaporation [30], [44]; 4) mixing; 5) stratification of the solution; 6) etch-product blocking of chemical flow [2]; 7) elapsed time from the start of the etch; 8) applied potential [2], [4], [5]; 9) illumination [45]; and 10) contamination. Etch-rate variation due to the material being etched is affected by 11) impurities in or on the material being etched [20], [46]; 12) microstructure [15], [47], [48]; and 13) film stress [49], [50]. Etch-rate variation due the layout and structure on the substrate is affected by 14) the distribution and fraction of surface area of the exposed target layer (loading) [2], [15], and 15) the structure geometry [13].

### III. THE PLASMA AND PLASMALESS-GAS-PHASE ETCHES

#### A. Purposes of the Etch Gases

Because many gases are used in more than one of the etches in Table II, each gas (in italics) and its purpose are presented here.

1) *Oxygen* ( $O_2$ ): dissociates into O radicals, which are more reactive. Oxygen has several purposes. Pure  $O_2$  plasmas are used to etch photoresist. In plasmas involving  $CF_4$ , O atoms displace F in the  $CF_4$  molecule, generating more free F [51]. This can both increase the etch rate and cause enough F to be present to allow the formation of C-F sidewall polymer films.

2) *Sulfur Hexafluoride* ( $SF_6$ ):  $SF_6$  is one source of very reactive F atoms that etch all of the materials in Table II except for aluminum. Fluorine atoms are not very selective, etching most of these materials at rates varying by less than a factor of 5. Molecular fluorine ( $F_2$ ) is not used for silicon etching because it is hazardous, and, for reasons not understood, it leaves rough surfaces [11], [52].

3) *Tetrafluoromethane* ( $CF_4$ , carbon tetrafluoride, Freon 14):  $CF_4$  is a source of F and also a source of C, both of which are required for C-F sidewall-polymer formation.

4) *Trifluoromethane* ( $CHF_3$ , Freon 23):  $CHF_3$  is another source of F and C, but with a lower ratio of F to C.

5) *Chlorine* ( $Cl_2$ ):  $Cl_2$  dissociates into Cl atoms, which are quite reactive. Like F, Cl etches most materials, including aluminum.

6) *Trichloromethane* ( $CHCl_3$ , chloroform):  $CHCl_3$  supplies chlorine for etching and carbon and chlorine for sidewall polymer formation [52].

7) *Boron Trichloride* ( $BCl_3$ ):  $BCl_3$  etches the native aluminum oxide film on aluminum. It also scavenges  $O_2$  and  $H_2O$  in the vacuum system, preventing oxide growth [53].

8) *Helium* (He): He can be used in plasma etching as a diluent and a plasma stabilizer [51]. Diluents give the user another process control variable. For example, an inert gas can be added to increase the total pressure while keeping the partial pressures of the other gases constant. In addition, some gas species can improve energy transfer from the "hot" electrons to reactive gas molecules (e.g., He enhances the dissociation of  $BCl_3$  [51]).

9) *Nitrogen* ( $N_2$ ):  $N_2$  is also used as a diluent.

10) *Hydrogen fluoride vapor* (HF): HF vapor evaporates rapidly from concentrated HF solutions. Like its liquid counterpart, it can be used for etching silicon oxides.

11) *Xenon Difluoride* ( $XeF_2$ ):  $XeF_2$  is supplied as granular crystals. At room temperature, it has an equilibrium vapor pressure of about 4.5 Torr [54].  $XeF_2$  supplies fluorine atoms in the plasmaless-gas-phase etching of silicon and some other materials.

12) *Other Gases*: Many other gases in various combinations have been used for plasma etching, as discussed in several of the references [1], [2], [51]–[53].

#### B. Information About Individual Plasma and Plasmaless Gas-Phase Etches

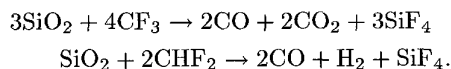
All of the plasma etches in Table II were done with recently cleaned chambers. The plasma etches are fairly anisotropic unless otherwise noted. The anisotropic plasma etches presented in this section have recipes that are based on the manufacturers' general recommendations for each machine, adapted to yield a useful compromise among a reasonably fast etch rate for the target material, fairly straight sidewalls, and selectivity over a photoresist mask layer.

In this section, the etches are grouped by reactive plasma species and target material. The reactions listed are summaries; the occurrence of a complicated series of subreactions, adsorptions, and possibly energetic ion involvement should be considered typical. Details of some of the reactions are given in the references.

Each etch is listed by its name from Table II in italics, which includes the gases, their flow rates, equipment brand and model number, power, pressure, electrode gap, and operating frequency.

The plasmaless-gas-phase etchants, HF vapor and  $XeF_2$ , are listed with the plasma etches because they are more similar to chemical-plasma etching than to wet etching: reactant and product flow occurs in the gas phase and there is a fresh flow of reactants to the etch surface.

1) *Fluorocarbon-Plasma Silicon-Dioxide Etches*: Reaction: It appears that  $CF_x$  ( $x \leq 3$ ) radicals chemisorb on the  $SiO_2$  and dissociate. The radicals supply carbon to form CO,  $CO_2$ , and  $COF_2$  gases from the oxygen in the film. They also supply fluorine to form  $SiF_4$  gas [55]. Overall reactions such as the following occur [2]:



$CF_4 + CHF_3 + He$  (90:30:130 sccm), Lam 590, 450 W, 2.8 T, gap = 0.38 cm, 13.56 MHz: Parallel-plate configuration, graphite electrode (others are aluminum), driven electrode area  $\approx 350 \text{ cm}^2$ .

Notes: This etch targets silicon dioxide, but also etches silicon nitride well. It can be patterned with photoresist (PR). This etch is anisotropic (fairly vertical sidewalls).

If total etch times longer than about 2 min are required, the etch is often broken up into several shorter times, giving the photoresist a chance to cool and thus erode less.

TABLE II

ETCHANT EQUIPMENT CONDITIONS	TARGET MATERIAL	Plasma- and Plasmas-Gas-Phase-Etch Rates for Micromachining and IC Processing (Å/min)															
		SC Si <100>	Poly n*	Poly undop	Wat Ox	Dry Ox	LTO undop	PSG unal	PSG amnl	Sioc Nitrid	Low-σ Nitrid	AU 2% Si	Sput Tung	Sput Ti	Sput Ti/W	OCG 820PR	Olin HnPR
CF <sub>4</sub> /CHF <sub>3</sub> /He (90:30:120 sccm) Lam 590 Plasma 450W, 2.8T, gap=0.38cm, 13.56MHz	Silicon oxides	W	1900	2100	4700	W	4500	7300	6200	1800	1900	-	W	W	W	2200	2600
CF <sub>4</sub> /CHF <sub>3</sub> /He (90:30:120 sccm) Lam 590 Plasma 850W, 2.8T, gap=0.38cm, 13.56MHz	Silicon oxides	W	2200	1700	6000	W	6400	7000	4200	3800	-	-	W	W	W	2600	2900
SF <sub>6</sub> /He (13:21 sccm) Technics PE II-A Plasma 100W, 250mT, gap=2.6cm, 50kHz sq. wave	Silicon nitrides	300	730	670	310	350	370	610	480	820	620	-	W	W	W	690	600
CF <sub>4</sub> /CHF <sub>3</sub> /He (10:5:10 sccm) Technics PE II-A Plasma 200W, 250mT, gap=2.6cm, 50kHz sq. wave	Silicon nitrides	1000	1900	W	730	710	730	W	940	1300	1100	-	W	W	W	690	600
SF <sub>6</sub> /He (175:50 sccm) Lam 480 Plasma 150W, 375mT, gap=1.35cm, 13.56MHz	Thin silicon nitrides	W	6400	7000	300	W	280	530	540	1300	870	-	W	W	W	1500	1400
SF <sub>6</sub> /He (180:400 sccm) Lam 480 Plasma 250W, 375mT, gap=1.35cm, 13.56MHz	Thick silicon nitrides	W	8400	9200	800	W	770	1500	1200	2800	2100	-	W	W	W	3400	3100
CF <sub>4</sub> /CHF <sub>3</sub> /He (45:15:60 sccm) Tegal Inline Plasma 701 125W, 200mT, 40°C	Thin silicon nitrides	W	1700	2800	1100	W	1100	1400	2800	2300	-	-	W	W	W	3400	3100
CF <sub>4</sub> /CHF <sub>3</sub> /He (45:15:60 sccm) Tegal Inline Plasma 701 100W, 300mT, 13.56MHz	Si-rich silicon nitrides	W	350	360	320	W	320	530	450	760	600	-	W	W	W	400	350
Cl <sub>2</sub> /He (180:400 sccm) Lam Rainbow 4420 Plasma 275W, 425mT, 40°C, gap=0.80cm, 13.56MHz	Silicon	W	5700	3200	8	-	60	230	140	560	530	W	W	W	-	3000	2700
HF/HCl <sub>2</sub> (70:70 sccm) Lam Rainbow 4420 Plasma 200W, 300mT, 40°C, gap=0.80cm, 13.56MHz	Aluminum	W	5000	6300	3700	380	-	0	0	870	26	W	W	W	-	350	300
Cl <sub>2</sub> /BCl <sub>3</sub> /CHCl <sub>3</sub> /N <sub>2</sub> (30:50:20:50 sccm) Lam 690 RIE 250W, 290mT, 60°C, 13.56MHz	Tungsten	W	4500	W	680	670	750	W	740	930	860	6000	W	W	-	6300	6300
SF <sub>6</sub> (80 sccm) Tegal Inline Plasma 701 200W, 150mT, 40°C, 13.56MHz	Descumming photoresist	W	5800	5400	1200	W	1200	1800	1500	2600	2300	-	2800	W	2400	2400	
O <sub>2</sub> (51 sccm) Technics PE II-A Plasma 50W, 300mT, gap=2.6cm, 50kHz sq. wave	Ashing Photoresist	-	0	0	0	0	0	0	0	0	0	0	0	0	0	0	3600
HF Vapor 1 cm over plastic dish Room temperature and pressure	Silicon oxides	-	0	0	660	W	780	2100	1500	10	19	A	0	A	-	P	0
XeF <sub>2</sub> Simple custom vacuum chamber Room temperature, 2.6 Torr	Silicon	4600	1900	1800	0	-	0	0	0	120	2	0	800	290	-	0	0

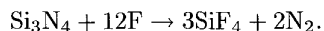
Notation: - test not performed; W=not performed, but known to work (≥ 100 Å/min); F=not performed, but known to be fast (≥ 10 Å/min); P=some of film peeled during etch or when rinsed; A=film was visibly attacked and roughened. Etch rates are all of a 4-inch wafer for the transparent films and half of the wafer for single-crystal silicon and the metals. Each area will vary with temperature and prior use plasma chamber, area of exposure of film, other materials present (e.g., photoresist), film impurities and microstructure, etc. Some variation should be expected.

$CF_4 + CHF_3 + He$  (90:30:130 sccm), Lam 590, 850 W, 2.8 T, gap = 0.38 cm, 13.56 MHz: Parallel-plate configuration, graphite electrode (others are aluminum), driven electrode area  $\approx 350 \text{ cm}^2$ .

Notes: This is a faster oxide etch than the lower-power etch above, but with lower selectivity to photoresist.

#### 2) Fluorine-Atom-Plasma Silicon-Nitride Etches:

Reaction: Fluorine atoms are adsorbed onto the surface one at a time. In a surface reaction, volatile products are formed. The overall reaction is [2]



The apparent activation energy for F-atom etching of  $Si_3N_4$  is about 0.17 eV [53].

$SF_6 + He$  (13:21 sccm), Technics PE II-A, 100 W, 250 mT, 50 kHz sq. wave: Parallel-plate configuration, fixed gap  $\approx 2.6$  cm, driven electrode area  $\approx 600 \text{ cm}^2$ . The chamber holds four wafers; the test was performed with one wafer.

Notes: This etch is used to plasma-etch silicon nitride. It can be masked with photoresist.

This etch exhibits a severe loading effect. It is not only affected by the number of wafers in the chamber, but also by the fraction of nitride surface area that is exposed. Furthermore, the etch rate varies with position in the chamber, so wafers should be rotated three or four times during an etch for uniformity.

Plasma etching, especially at higher power, heats the chamber, which can affect etch rates and thus selectivity. During all Technics PE II-A tests, the plate temperature varied from 20 to 30°C.

$CF_4 + CHF_3 + He$  (10:5:10 sccm), Technics PE II-A, 200 W, 250 mT, 50 kHz sq. wave: Parallel-plate configuration, fixed gap  $\approx 2.6$  cm, driven electrode area  $\approx 600 \text{ cm}^2$ . The chamber holds four wafers; the test was performed with one wafer.

Notes: This silicon nitride plasma etch uses fluorocarbons rather than  $SF_6$  as the source of F atoms.

$SF_6 + He$  (175:50 sccm), Lam 480, 150 W, 375 mT, gap = 1.35 cm, 13.56 MHz: Parallel-plate configuration, driven electrode area  $\approx 350 \text{ cm}^2$ .

This silicon nitride plasma etch is in a single-wafer system. The slower etch rate than the etch listed below is intended for thin nitride films. It can be patterned with photoresist. The etch is anisotropic (fairly vertical sidewalls).

$SF_6 + He$  (175:50 sccm), Lam 480, 250 W, 375 mT, gap = 1.35 cm, 13.56 MHz: Parallel-plate configuration, driven electrode area  $\approx 350 \text{ cm}^2$ .

Notes: This silicon nitride plasma etch is faster and therefore useful for thicker nitride films. It can be patterned with photoresist.

If total etch times longer than about 2 min are required, the etch is often broken up into several shorter times, giving the PR a chance to cool and thus erode less.

$SF_6$  (25 sccm), Tegal Inline Plasma 701, 125 W, 200 mT, 13.56 MHz: Parallel-plate configuration, fixed gap  $\approx 3.8$  cm, driven electrode area  $\approx 250 \text{ cm}^2$ .

Notes: This slower etch is intended for thinner, stoichiometric silicon nitride films.

$CF_4 + CHF_3 + He$  (45:15:60 sccm), Tegal Inline Plasma 701, 100 W, 300 mT, 13.56 MHz: Parallel-plate configuration, fixed gap  $\approx 3.8$  cm, driven electrode area  $\approx 250 \text{ cm}^2$ .

Notes: This etch has a different gas chemistry than the previous etch, aimed at thicker, silicon-rich nitride films.

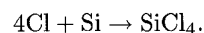
#### 3) Plasma Silicon Etches:

$Cl_2 + He$  (180:400 sccm), Lam Rainbow 4420, 275 W, 425 mT, 40°C, gap = 0.80 cm, 13.56 MHz: Parallel-plate configuration, driven electrode area  $\approx 390 \text{ cm}^2$ .

Notes: This is an anisotropic silicon plasma etch. An  $SF_6$  step prior to this one is typically used to break through the native oxide.

This etch has been used to micromachine 80- $\mu\text{m}$ -deep trenches with fairly vertical sidewalls [56].

Reaction: Chlorine atoms are chemisorbed one at a time on the silicon surface, eventually forming volatile  $SiCl_4$  [53]. The overall reaction is



Chlorine etching of undoped silicon occurs very slowly in the absence of ion bombardment [53]. Unlike F-atom silicon etches, Cl- and Br-based etches tend to be vertical [51].

As the Fermi level rises, the energy barrier for charge transfer of chemisorbed Cl, a step in the etch process, falls [53]. Thus, *p*-type doping slows etching while *n*-type doping accelerates it.

Chlorine-based plasma etch rates of single-crystal silicon can also depend on crystallographic orientation. Kinoshita and Jinno found that, with  $CCl_4 + He$  plasmas, the {100} and {110} planes could be etched faster than the {111} planes [57]. The selectivity was not, however, as great as with KOH- or EDP-based etches.

$HBr + Cl_2$  (70:70 sccm), Lam Rainbow 4420, 200 W, 300 mT, 40°C, gap = 0.80 cm, 13.56 MHz: Parallel-plate configuration, driven electrode area  $\approx 390 \text{ cm}^2$ .

Notes: This is another anisotropic silicon plasma etch, with better selectivity of silicon over oxide.

Reaction: Bromine atoms probably react with silicon in a manner similar to chlorine as described above.

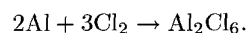
#### 4) Plasma Metal Etches:

$Cl_2 + BCl_3 + CHCl_3 + N_2$  (30:50:20:50 sccm), Lam 690, 250 W, 250 mT, 60°C, 13.56 MHz: Parallel-plate grounded-chuck configuration, fixed gap  $\approx 2.5$  cm, driven electrode area  $\approx 350 \text{ cm}^2$ .

Notes: This is an anisotropic aluminum plasma etch due to the sidewall inhibitor formed from the  $CHCl_3$  [52].

Due to poor selectivity, for thick layers of Al, thicker photoresist, plasma-hardened PR, or a more-durable masking layer must be used. The higher temperature is used to keep the etch product volatile so that it leaves the wafer [2] and does not coat the chamber or exhaust plumbing.

Reaction: The dominant overall reaction below 200°C [52] is



$Cl_2$  rather than Cl appears to be the main etchant [52]. The etch product becomes  $AlCl_3$  at higher temperatures [11], [52].

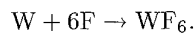
All aluminum etches in the Berkeley Microlab are followed by airlock plasma processing:  $\text{CF}_4 = 90$  sccm,  $\text{O}_2 = 10$  sccm,  $P = 400$  W, for 1 min. The airlock recipe is not intended to do any etching. It replaces the chlorine in the residual  $\text{Al}_2\text{Cl}_6$  with fluorine. If this step were not performed, the chlorine would form hydrochloric acid upon exposure to atmospheric moisture, causing later corrosion of the aluminum.

*SF<sub>6</sub> (80 sccm), Tegal Inline Plasma 701, 200 W, 150 mT, 40 °C, 13.56 MHz:* Parallel-plate configuration, fixed gap  $\approx 3.8$  cm, driven electrode area  $\approx 250$  cm<sup>2</sup>. Grounded chuck.

Notes: This tungsten plasma etch is fairly isotropic.  $\text{CF}_4$  added to the feed gas increases anisotropy as sidewall polymers form, but slows the etch rate.

The chuck is heated to enhance the etch rate.

Reaction: The overall reaction is



5) *Oxygen-Plasma Photoresist Etches:* Reaction: Oxygen atoms “burn” or “ash” (a misnomer) the organic photoresist, forming mostly  $\text{H}_2\text{O}$ ,  $\text{CO}_2$ , and  $\text{CO}$  [53]. Activation energies for O-atom etching of photoresist have been measured in the range of 0.22 to 0.65 eV [53]. Below 60 °C, PMMA has an activation energy of about 0.2 eV [52].

*O<sub>2</sub> (51 sccm), Technics PE II-A, 50 W, 300 mT, 50 kHz sq. wave:* Parallel-plate configuration, gap  $\approx 2.6$  cm, driven electrode area  $\approx 600$  cm<sup>2</sup>. The chamber holds four wafers; the test was performed with one wafer.

Notes: This plasma-processing step is used for “descumming” (removing undesired thin layers) of freshly developed photoresist, typically for one minute. Unbaked OCG 820 PR was removed 6% faster than hardbaked PR during a descum test.

*O<sub>2</sub> (51 sccm), Technics PE II-A, 400 W, 300 mT, 50 kHz sq. wave:* Parallel-plate configuration, fixed gap  $\approx 2.6$  cm, driven electrode area  $\approx 600$  cm<sup>2</sup>. The chamber holds four wafers; the test was performed with one wafer.

Notes: This oxygen plasma is used to ash (strip) photoresist for 5–10 min. A power of 300 W is also often used. It has been argued that lower power is better because there is less possibility of plasma hardening during stripping and of damage to MOS devices.

A loading effect, in which the etch rate decreases when there is more photoresist surface area, has been observed. In a 400 W PR stripping test, ashing four wafers at the same time was 23% slower than ashing one alone.

#### 6) *Plasmless HF-Vapor Silicon-Dioxide Etch:*

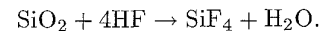
*HF Vapor, 1 cm over plastic dish, Room temperature and pressure:* Notes: Like liquid-based HF etches, HF vapor etches silicon dioxide. It has been used to remove native oxide from silicon before the growth of epitaxial silicon [58] and other processes such as the  $\text{XeF}_2$  etching of silicon.

In these tests, the  $\text{HF}/\text{H}_2\text{O}$  vapor condensed into droplets on the surfaces of the oxide samples during the 1-min etch, causing faster etching where these droplets had formed. This nonuniform etching can be greatly reduced by etching in “pulses,” removing the wafer from the vapor before droplets form and allowing it to evaporate.

HF vapor may also be suitable for vapor-phase removal of a sacrificial oxide layer for micromechanical fabrication; however, caution should be used with photoresist masks, which may peel (in these tests, the photoresist peeled when the wafers were rinsed).

In these tests, thermal oxide was etched at one third the rate of unannealed PSG. Other researchers have found that this selectivity goes up by two orders of magnitude when the wafers are heated to 50 °C [59].

Reaction: The overall reaction is [58]



Water is assumed to catalyze the reaction [58], so a pure HF vapor may have a much slower etch rate than that over the 49%  $\text{HF}/51\%$   $\text{H}_2\text{O}$  used here. There is a brief incubation time at the beginning of the etch during which water molecules condense on the surface to be etched [58].

#### 7) *Plasmless XeF<sub>2</sub> Silicon Etch*

*XeF<sub>2</sub>, Simple custom vacuum chamber, room temperature, 2.6 Torr:* Notes:  $\text{XeF}_2$  was first synthesized in 1962 [60] and has been the subject of several papers on silicon etching [54], [61], but was only recently “rediscovered” for its suitability for micromachining [62].

$\text{XeF}_2$  gas has the unusual capability to etch silicon at a significant rate without requiring a plasma to generate reactive species. As with chemical-plasma etching [52], etching is isotropic. The etched surface in deeply etched bulk silicon has been reported to have a roughness of several micrometers [62].

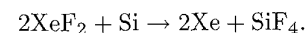
$\text{XeF}_2$  has been used to micromachine free-standing structures made of aluminum and polysilicon protected by a layer of oxide [62].  $\text{XeF}_2$  has the advantage over wet silicon etchants of gently etching without applying capillary forces, and the advantage over plasma etches of being extremely selective over almost all of the traditional masking layers, such as silicon dioxide, some silicon nitrides, and photoresist.

Because the native oxide on silicon surfaces completely stops etching, the silicon etch samples in these etch-rate tests were dipped in 10:1 HF, rinsed, and spun dry a few minutes before the etch rate tests. A period of 18 h in a wafer box in room air was found to be sufficient to grow enough native oxide on doped polysilicon to stop etching completely.

The etch rate has been reported to be extremely load-dependent [62], and measured values in our lab are as low as 11 nm/min (for some regions of the wafer) when an entire 4-in. wafer is exposed to the  $\text{XeF}_2$ , up to 10  $\mu\text{m}/\text{min}$  for small chips of silicon.

The etching apparatus used for these etch-rate measurements allowed exposure of a 4-in. wafer to a 3.5-liter volume of  $\text{XeF}_2$  at its room-temperature equilibrium pressure for 30 s, after which the etch chamber was pumped down for 30 s. For etches of total time longer than 30 s (all data here are for one minute of etch time), this “pulsed-etching” cycle was repeated.

Reaction:  $\text{XeF}_2$  molecules are physisorbed on the silicon surface [61] and dissociate to release volatile xenon atoms, while the fluorine atoms (not  $\text{F}_2$  [54]) remain to react with the silicon to form volatile  $\text{SiF}_4$ . The overall reaction is



The limiting step in the etching process appears to be the supply of fluorine atoms to the reaction site. Different steps in the supply processes dominate at different temperatures, causing a minimum in the etch rate of silicon as a function of temperature at around 410 K [61]. Ibotson *et al.* hypothesize that the etch rate increases below 410 K because the surface coverage of physisorbed  $\text{XeF}_2$  is greater (the  $\text{XeF}_2$  is less volatile), and this is the etch-rate-limiting step. When the etch-rate data at these lower temperatures were fitted to an Arrhenius equation multiplied by the density of  $\text{XeF}_2$ , the effective activation energy was found to be negative at  $-0.14$  eV (which corresponds to a positive activation energy for desorption). Above 410K the surface coverage is lower, but direct impact dissociation greatly increases the supply of fluorine atoms for the reaction. The effective activation energy for these higher temperatures was found to be 0.26 eV.

The etch rate of silicon has been observed to be proportional to the density of  $\text{XeF}_2$  molecules for pressures below 0.5 Torr, rising less than linearly at higher pressures [61]. The etch rate has been found to be proportional to the incident flux of  $\text{XeF}_2$  under flow that is force-blown perpendicular to the surface.

While according to several references,  $\text{XeF}_2$  alone does not etch silicon dioxide and nitride (to the contrary, stoichiometric silicon nitride was etched slowly in our tests), it does etch these dielectrics in the presence of ion or electron bombardment and under UV radiation [54]. This may help to explain why fluorine atoms are nonselective in plasma etches.

### C. Plasma-Etch-Rate Variation

Assuming that an etch chemistry (reactive gases and additives), reactor configuration (grounded or driven wafer holder), and RF-power supply (which sets the frequency and power range) have been selected, we have identified a number of factors that can affect plasma-etch rates. These sources of etch-rate variation can be divided into three categories: the etch setup, the material being etched, and the layout and structure on the substrate. The most significant effects on plasma-etch rate in each category are as follows (due to space constraints, the reader is referred to the references for detailed information on these sources of etch-rate variation).

Etch-rate variation due to the etch setup is a function of 1) power [52]; 2) pressure [52], [63]; 3) gas-flow rates [53]; 4) temperature [52], [53]; 5) film blocking of chemical flow [1], [64]; 6) elapsed time from the start of the etch; 7) materials present in the plasma chamber [2]; 8) changes in the etch chamber (e.g., wear of the electrode); and 9) contamination. Etch-rate variation due to the material being etched is affected by 10) impurities in or on the material being etched [53]; 11) microstructure; and 12) film stress. Etch rates also vary as a consequence of the layout and structure due to the 13) distribution and fraction of surface area of the target layer exposed (loading effect) [15]; and 14) specimen structure geometry.

## IV. SAMPLE PREPARATION/MEMS APPLICATIONS

Most of the materials listed in the etch-rate tables are frequently used in the U. C. Berkeley Microfabrication Laboratory for micromachining and IC fabrication. The materials are

discussed in the following list, which shows the abbreviated material names from Tables I and II in italics. The refractive index (RI) of each transparent film, used in thickness measurements, is listed. Preparation methods for the films are given, along with some MEMS applications and comments.

*SC Si <100>*: Single-crystal silicon, lightly doped with boron, with <100> orientation.

Single-crystal silicon, in the form of wafers, is the standard starting material for bulk micromachining [65].

*Poly n<sup>+</sup>*: In-situ heavily n-doped polycrystalline silicon. RI = 3.97.

Deposited on a wafer with thermal oxide already on it to enable interferometric thickness measurements. Deposited in a Tylan LPCVD furnace with the recipe  $\text{SiH}_4 = 120$  sccm,  $\text{PH}_3 = 1$  sccm,  $605^\circ\text{C}$ ,  $p = 300$  mT. No anneal.

This deposition temperature and pressure were chosen to yield a low, tensile residual stress [47] suitable for micromachined beams and shells.

*Poly*, both doped and undoped, is a common MEMS structural material.

*Poly undop*: Undoped polycrystalline silicon. RI = 3.97.

Deposited on a wafer with thermal oxide already on it to enable interferometric thickness measurements. Deposited in a Tylan LPCVD furnace with the recipe  $\text{SiH}_4 = 100$  sccm,  $605^\circ\text{C}$ ,  $p = 300$  mT. No anneal.

*Wet Ox*: Silicon dioxide thermally grown in water vapor. RI = 1.46.

Grown in a Tylan atmospheric-pressure furnace with the recipe  $1100^\circ\text{C}$ ,  $\text{O}_2$  carrier gas at 200 sccm,  $\text{H}_2\text{O}$  vapor at a pressure just below 1 atm (the water source is at  $98^\circ\text{C}$ ), and a total pressure of 1 atm, followed by a 20-min  $\text{N}_2$  anneal at  $1100^\circ\text{C}$ .

Thermal oxide has been used for thin sacrificial layers and for sealing cavities [66].

*Dry Ox*: Silicon dioxide thermally grown in dry oxygen. RI = 1.46.

Grown in a Tylan atmospheric-pressure furnace with the recipe  $1100^\circ\text{C}$ ,  $\text{N}_2 = 200$  sccm,  $\text{O}_2 = 4000$  sccm,  $p = 1$  atm, followed by a 30-minute  $\text{N}_2$  anneal at  $1100^\circ\text{C}$ .

Dry oxidation, with its slow growth rate, can be used for very thin oxide layers of controlled thickness.

*LTO undop*: Undoped, annealed low-temperature oxide. RI = 1.46.

Deposited in a Tylan LPCVD furnace with the recipe  $\text{SiH}_4 = 60$  sccm,  $\text{O}_2 = 90$  sccm,  $\text{PH}_3 = 0$  sccm (no doping),  $450^\circ\text{C}$ ,  $p = 300$  mT. Annealed in  $\text{N}_2$  in a Tylan atmospheric-pressure furnace at  $1000^\circ\text{C}$  for 60 min.

LTO is used as a sacrificial layer, but it has a much slower etch rate than that of PSG in HF-based etches. It is only etched slightly faster than thermal oxides.

*PSG unanl*: Doped phosphosilicate glass with no anneal. RI = 1.47.

Deposited in a Tylan LPCVD furnace with the recipe  $\text{SiH}_4 = 60$  sccm,  $\text{O}_2 = 90$  sccm,  $\text{PH}_3 = 10.3$  sccm (considered a high doping level),  $T = 450^\circ\text{C}$ ,  $p = 300$  mT.

Unannealed PSG has a much higher etch rate than annealed PSG. It has, however, been observed in the Berkeley Microlab to outgas during subsequent high-temperature steps, causing

bubbling in overlying films, so it is not used as frequently as annealed PSG.

*PSG anml:* Doped, annealed phosphosilicate glass. RI = 1.48.

Deposited in a Tylan LPCVD furnace under the same conditions as the unannealed PSG above, then annealed in N<sub>2</sub> in a Tylan atmospheric-pressure furnace at 1000 °C for 60 min. This PSG has about 5.5 molar percent P<sub>2</sub>O<sub>5</sub> in SiO<sub>2</sub>.

Oxides, usually chemical-vapor-deposited rather than thermally grown, are common sacrificial materials in micromachining. PSG (a doped LTO) etches much faster than undoped LTO in HF solutions, and is therefore preferred in structures requiring significant undercut.

*Stoic Nitrid:* Stoichiometric silicon nitride (Si<sub>3</sub>N<sub>4</sub>). RI = 1.99.

Deposited in a Tylan LPCVD furnace with the recipe NH<sub>3</sub> = 75 sccm, SiH<sub>2</sub>Cl<sub>2</sub> = 25 sccm,  $p = 200$  mT,  $T = 800$  °C.

Stoichiometric silicon nitride is used in masking and for layers that are not free-standing. High tensile residual stress precludes its use in free-standing structures.

*Low- $\sigma$  Nitrid:* Low-stress silicon nitride (silicon-rich Si <sub>$x$</sub> N <sub>$y$</sub> ). RI = 2.18.

Deposited in a Tylan LPCVD furnace with the recipe NH<sub>3</sub> = 16 sccm, SiH<sub>2</sub>Cl<sub>2</sub> = 64 sccm,  $p = 300$  mT,  $T = 835$  °C.

Low-stress silicon nitride is used for optically transparent membranes and shells [67], [68]. The refractive index rises with silicon content.

*Al/2% Si:* Sputtered aluminum with 2% silicon in the target.

Deposited in a CPA 9900 Sputtering System with the recipe  $p = 4.5$  kW, track speed = 20 cm/min,  $p = 6$  mT. The substrate temperature was not controlled during sputtering and rose above room temperature.

Aluminum is used for interconnects and as a structural material in conjunction with organic sacrificial layers such as polyimide [5], [6].

*Sput Tung:* Sputtered tungsten.

Deposited in a CPA 9900 Sputtering System with the recipe  $P = 4.5$  kW, track speed = 10 cm/min,  $p = 6$  mT. The substrate temperature was not controlled during sputtering and rose above room temperature.

Tungsten, both sputtered (with thermal anneal for stress control) and CVD, is used for interconnects that can withstand high-temperature processing [69] as well as for a structural material [70].

*Sput Ti:* Sputtered titanium.

Deposited in a CPA 9900 Sputtering System with the recipe  $P = 4.5$  kW, track speed = 10 cm/min,  $p = 6$  mT. The substrate temperature was not controlled during sputtering and rose above room temperature.

Titanium, being very reactive, is one of the few metals with good adhesion to oxide and nitride (aluminum and chromium are others). It is used as an adhesion layer for other, less-adhesive films, such as tungsten and gold.

*Sput Ti/W:* Sputtered 90% titanium/10% tungsten alloy.

Deposited in a Balzers 450 Sputtering System.

Ti/W is used as an adhesion layer for sputtered and CVD tungsten.

*OCG 820PR:* OCG 820 (G-line sensitive) positive photoresist. RI = 1.65.

Spun on using an SVG photoresist coater at 6000 rpm for 30 s. Hardbaked 30 min at 120 °C (experiments showed that baking for over 1 day had little difference on etch rate from 30 min of hardbaking).

For situations requiring a more durable resist, hardbaking at a higher temperature (up to 180 °C), plasma hardening, or deep UV hardening can be done [1].

Photoresist hardening can also occur unintentionally during plasma etching. Difficult-to-remove PR can usually be removed in an oxygen plasma, piranha etch, or a commercial photoresist stripper (e.g., J. T. Baker PRS-2000 at 90 °C).

In addition to masking, various photoresists [71] and other polymers [5], [6] have been used as sacrificial layers in micromachining and as liftoff layers in patterning [1]. Photoresist has been etched with acetone, but oxygen plasmas are most common for micromachining removal of polymers, largely because no liquid is involved (liquid capillary forces cause free-standing structures to be pulled down as the liquid dries [3]).

*Olin HntPR:* Olin Hunt 6512 (I-line-sensitive) positive photoresist.

Spun on using an SVG photoresist coater. Hardbaked 30 min at 120 °C. RI = 1.63.

## V. ETCH-RATE MEASUREMENT TECHNIQUES

*Transparent films (polysilicon, oxides, nitrides, photoresists)* were each coated over an entire 100-mm (4-in.) wafer and etched without patterning. While 100% wafer area is rarely etched at once in MEMS and IC processing, a full-wafer etch was carried out to avoid effects caused by the presence of different materials in the etch. The film thicknesses were measured interferometrically with a NanoSpec AFT interferometric film-thickness-measurement system, which was found to give very repeatable measurements. Refractive indexes (RI's) were determined by ellipsometry and verified with the NanoSpec. These RI's are listed in the samples section of this report. (The apparent RI of the low-stress nitride films was significantly different when measured using the NanoSpec than by using the ellipsometer. We give the ellipsometer RI, which most often agrees with published data.)

Five locations on each wafer were measured before each etch, the films were etched, and then the same five locations (to within a few millimeters) were measured again. The average of the differences of these five points, divided by the etch time, determined the etch rate.

*Opaque films (single-crystal silicon, metals)* were etched several different ways to allow for measurement. Most of the metal etches were done with a photoresist masking layer covering about 50% of the wafer. Previously patterned tungsten on a film of silicon nitride was used for tungsten in KOH and in the oxygen plasmas. Single-crystal silicon (SCS) with a nitride mask was used for SCS in KOH.

Five step heights distributed around the wafer were measured with a Tencor Alphastep 200 step profiler, the film

was etched, then the same steps (to within a few tenths of a millimeter) were measured again. The average step-height difference (and the etch rate of the masking layer, if nonzero) were used to determine the etch rate of the film.

*Wet etches* having moderately fast rates ( $>1000 \text{ \AA}/\text{min}$ ) were done for one minute (even less for a few very rapid etches). Slower wet etches were done for at least 10 min to get a more accurate measurement. Materials with reported etch rates slower than  $10 \text{ \AA}/\text{min}$  were etched for at least 30 min.

*Plasma and plasmaless-gas-phase etching* were done for 1 min (or, for a few very rapid etches, for 30 s), with one wafer in the etch chamber. Care was taken to avoid plasma-hardening effects with the photoresist samples (fresh samples were used for each etch test).

*Accuracy of measurements:* An etch rate is listed if the computed standard deviation was smaller than the average rate. In cases where the standard deviation was larger than the average (or the surfaces were very rough when Alphastep measurements were used) indicating significant variation across the wafer, an upper limit equal to the average plus one standard deviation is given (e.g.,  $<50 \text{ \AA}/\text{min}$ ). Etch rates of zero are recorded if the films were *thicker* after the etch, as often happened with photoresist in wet etches (the photoresist absorbed water). In a few cases, such as PR in acetone, the entire film was removed in a very short time; a lower limit is listed for these etch rates (e.g.,  $>44 \text{ k\AA}/\text{min}$ ). The measurements are rounded to two significant figures. The results are estimated to be accurate to within  $\pm 5\%$  or  $\pm 5 \text{ \AA}/\text{min}$ , whichever is smaller.

## VI. ETCH-RATE RESULTS

### A. Etch-Rate Tables

The etch-rate data is divided into two tables. Table I covers wet etches; Table II deals with plasma and plasmaless-gas-phase etches. Etches are grouped by target material. Etch rates are reported in the commonly used units of angstroms per minute.

For each combination of material and etchant (e.g.,  $n^+$  poly and silicon etchant), up to three values are listed. For 317 of the combinations, the top value is the etch rate measured by the authors using fresh solutions, clean chambers, controlled temperatures, etc. (e.g.,  $3100 \text{ \AA}/\text{min}$  for  $n^+$  poly in wet silicon etchant).

Recognizing that etch rates vary due to many process factors (e.g., previous use of solution or plasma chamber, temperature, area of wafer exposed), we have included further data in the tables on the observed range of etch rates to provide an idea of the range of etch rates that might be expected. When available, the middle and bottom numbers are the slowest and fastest etch rates, respectively, observed by the authors and others in our laboratory during the past five years, using fresh and used solutions, "clean" and "dirty" plasma chambers, and looser temperature control (e.g.,  $1200$  and  $6000 \text{ \AA}/\text{min}$  for  $n^+$  poly in silicon etchant). These observed variation ranges for etch rates are quite wide in a number of cases. Wider ranges usually occur for etches performed by many lab users. In some

instances, the observed variation is small. This may either indicate that the etch is particularly repeatable or, perhaps, that only a few results were reported by other lab users. Therefore, an etch with a narrow range of reported rates in the tables should not be interpreted as being particularly repeatable.

In some cases, an etch rate was not measured but something else significant happened. For cases in which the film (usually photoresist) peeled, a "P" is entered in the tables. When the material was not etched significantly but was attacked forming a rough surface, an "A" is listed.

Etch-rate tests for many of the combinations of materials and etches in the tables were not performed, often due to cross-contamination concerns in the plasma-etching equipment. When known, based on both published reports and local experience with the chemicals and materials involved, we have included in Tables I and II whether 70 of these combinations support an etch rate of at least  $100 \text{ \AA}/\text{min}$  (denoted by a "W" for "works" in the tables), and whether the etch is very fast (at least  $10 \text{ k\AA}/\text{min}$ , denoted by an "F").

Because of their strong dependencies on many factors, *etch rates should not be expected to exactly match those listed in Tables I and II. The tabulated etch rates are to be understood as being order-of-magnitude repeatable and valid when considering relative etch rates for different materials.*

### B. Discussion of Etch-Rate Data

Several conclusions can be drawn from the data in the etch-rate tables. Some are considered common knowledge among those familiar with micromachining and semiconductor processing or are expected from the literature on the subject.

Wet etches tend to be more selective than plasma etches. Plasma etches using  $\text{SF}_6$ ,  $\text{CF}_4$ , or  $\text{CHF}_3$ , which supply fluorine radicals, are particularly nonselective.

For hydrofluoric-acid-based etching of various types of silicon dioxide, we find that for weaker concentrations of HF (going from 25:1 to 10:1), the etch rate increases almost linearly with concentration, but rises much faster going to concentrated HF. No difference in the etch rates of wet and dry thermally grown silicon dioxide is observed.

Annealing PSG greatly slows its etch rate in most wet etches, but does not affect the plasma-etch rate significantly. Annealed, undoped LTO etches much more slowly in all of the wet etches, and slightly more slowly in the plasma etches than the annealed PSG (doped LTO), approaching the slow etch rate of the thermal oxides.

$N^+$  polysilicon etches faster than undoped poly in the silicon wet etchant and in the chlorine-based plasma, but the two etch at roughly the same rate in the fluorine-based plasmas.

Stoichiometric silicon nitride etches at the same rate or faster than the silicon-rich low-stress nitride in all of the etches except HF vapor.

Tungsten is removed slowly or not at all in all of the wet etches tested, including HF and KOH solutions, making it a candidate for a structural material in micromachined devices.

Titanium is etched so much faster than most silicon oxides in HF solutions that it is possible to stop a titanium etch on oxide.

The etch rates of the two brands of positive photoresist studied are within 15% of each other in most of the etches, with neither photoresist always being removed more slowly or rapidly. In results not reported in the table, we varied the hardbake time of the OCG 820 from its standard 30 min to 1 h and 1 day. Surprisingly, this had a negligible effect on the removal rate.

The oxygen plasmas, intended for descumming and stripping photoresist, attack only photoresist.

Piranha, intended for cleaning metals and organics from wafers, attacks only the metals and photoresists in these tests.

Xenon difluoride selectively etches silicon, as well as titanium and tungsten. It unexpectedly (but repeatedly) also etches stoichiometric silicon nitride, but not silicon-rich nitride.

#### ACKNOWLEDGMENT

The authors thank K. Voros of the U. C. Berkeley Microfabrication Laboratory, C. Keller and M. Houston of the Berkeley Sensor & Actuator Center, and N. Cheung of Electrical Engineering and Computer Sciences, all at the University of California at Berkeley, for reviewing this paper and providing constructive criticism. They also thank R. Hamilton of the Berkeley Microlab for providing information about etching equipment.

#### REFERENCES

- [1] S. Wolf and R. N. Tauber, *Silicon Processing for the VLSI Era*. Sunset Beach, CA: Lattice, 1986, vol. 1.
- [2] W. R. Runyan and K. E. Bean, *Semiconductor Integrated Circuit Processing Technology*. Reading, MA: Addison-Wesley, 1990.
- [3] C. H. Mastrangelo and C. H. Hsu, "Mechanical stability and adhesion of microstructures under capillary forces—Part II," *IEEE J. Microelectromech. Syst.*, vol. 2, no. 1, pp. 44–55, Mar. 1993.
- [4] G. T. Mulhern, D. S. Soane, and R. T. Howe, "Supercritical carbon dioxide drying of microstructures," in *Tech. Dig. 7th Int. Conf. on Solid-State Sensors and Actuators (Transducers '93)*, Yokohama, Japan, June 1993, pp. 296–299.
- [5] J. B. Sampsell, "The digital micromirror device and its application to projection displays," in *Tech. Dig. 7th Int. Conf. on Solid-State Sensors and Actuators (Transducers '93)*, Yokohama, Japan, June 1993, pp. 24–27.
- [6] C. W. Stormont, D. A. Borkholder, V. Westerlind, J. W. Suh, N. I. Maluf, and G. T. A. Kovacs, "Flexible, dry-released process for aluminum electrostatic actuators," *IEEE J. Microelectromech. Syst.*, vol. 3, no. 3, pp. 90–96, Sept. 1994.
- [7] R. C. Weast, Ed., *CRC Handbook of Chemistry and Physics*, 66th ed. Boca Raton, FL: CRC, 1985 pp. B-67–B-161.
- [8] G. L. Clark, Ed., *The Encyclopedia of Chemistry*. New York: Reinhold, 1966.
- [9] G. G. Hawley, *The Condensed Chemical Dictionary*, 8th Ed. New York: Van Nostrand Reinhold, 1971.
- [10] J. W. Mellor, *A Comprehensive Treatise on Inorganic and Theoretical Chemistry*. London: Longmans, Green and Co., 1927, vol. 2.
- [11] J. L. Vossen and W. Kern, Eds., *Thin Film Processes*. New York: Academic, 1978, ch. V-1.
- [12] R. L. Alley, G. J. Cuan, R. T. Howe, and K. Komvopoulos, "The effect of release-etch processing on surface microstructure stiction," in *Tech. Dig. IEEE Solid-State Sensor and Actuator Workshop*, Hilton Head, SC, June 1992, pp. 202–207.
- [13] D. J. Monk, "Controlled structure release for silicon surface micromachining," Ph.D. dissertation, Chem. Eng., Univ. of California, Berkeley, 1993.
- [14] K. S. Leboutitz, R. T. Howe, and A. P. Pisano, "Permeable polysilicon etch-access windows for microshell fabrication," in *Tech. Dig. 8th Int. Conf. on Solid-State Sensors and Actuators (Transducers '95)*, Stockholm, Sweden, June 1995, pp. 224–227.
- [15] S. K. Ghandi, *VLSI Fabrication Principles*. New York: Wiley, 1983, ch. 9.
- [16] H. Kikyuama, N. Miki, K. Saka, J. Takano, I. Kawanabe, M. Miyashita, and T. Ohmi, "Principles of wet chemical processing in ULSI microfabrication," *IEEE Trans. Semicond. Manufact.*, vol. 4, no. 1, pp. 26–35, Feb. 1991.
- [17] J. S. Judge, "A study of the dissolution of SiO<sub>2</sub> in Acidic Fluoride Solutions," *J. Electrochem. Soc.*, vol. 118, no. 11, pp. 1772–1775, Nov. 1971.
- [18] C. A. Deckert, "Etching of CVD Si<sub>3</sub>N<sub>4</sub> in acid fluoride media," *J. Electrochem. Soc.*, vol. 125, no. 9, pp. 320–323, Feb. 1978.
- [19] G. I. Parisi, S. E. Haszko, and G. A. Rozgonyi, "Tapered windows in SiO<sub>2</sub>: The effect of NH<sub>4</sub>F:HF dilution and etching temperature," *J. Electrochem. Soc.*, vol. 124, no. 6, pp. 917–921, June 1977.
- [20] A. S. Tenny and M. Ghezzi, "Etch rates of doped oxides in solutions of buffered HF," *J. Electrochem. Soc.*, vol. 120, no. 8, pp. 1091–1095, Aug. 1973.
- [21] R. A. Haken, I. M. Baker, and J. D. E. Beynon, "An investigation into the dependence of the chemically-etched edge profiles of silicon dioxide on etchant concentration and temperature," *Thin Solid Films*, vol. 18, no. 1, pp. S3–S6, Oct. 1973.
- [22] J. T. Baker, Inc., "Product Specifications for Product No. 5192, Buffered Oxide Etch, 5:1," J. T. Baker, Inc., Phillipsburg, NJ, 1993, tech. support, June 7, 1995.
- [23] W. van Gelder and V. E. Hauser, "The etching of silicon nitride in phosphoric acid with silicon dioxide as a mask," *J. Electrochem. Soc.*, vol. 114, no. 8, pp. 869–872, Aug. 1967.
- [24] H. Robbins and B. Schwartz, "Chemical etching of silicon I," *J. Electrochem. Soc.*, vol. 106, pp. 505–508, 1961.
- [25] P. K. Ko, formerly of Dept. EECS, Univ. of California, Berkeley, personal communication, June 11, 1996.
- [26] D. R. Turner, "On the mechanism of chemically etching germanium and silicon," *J. Electrochem. Soc.*, vol. 107, no. 10, pp. 810–816, Oct. 1960.
- [27] Fisher Chemical/Fisher Scientific, "Bottle label of potassium hydroxide, solid," Fisher Chemical, Fair Lawn, NJ, 1996.
- [28] D. L. Kendall, "A new theory for the anisotropic etching of silicon and some underdeveloped chemical micromachining concepts," *J. Vac. Sci. Technol. A*, vol. 8, no. 4, pp. 3598–3605, Jul./Aug. 1990.
- [29] H. Seidel, L. Csepregi, A. Heuberger, and H. Baumgartel, "Anisotropic etching of crystalline silicon in alkaline solutions, II. Influence of dopants," *J. Electrochem. Soc.*, vol. 137, no. 11, pp. 3626–3632, Nov. 1990.
- [30] ———, "Anisotropic etching of crystalline silicon in alkaline solutions, I. Orientation dependence and behavior of passivation layers," *J. Electrochem. Soc.*, vol. 137, no. 11, pp. 3612–3626, Nov. 1990.
- [31] O. Tabata, R. Asahi, H. Funabashi, K. Shimoka, and S. Sugiyama, "Anisotropic etching of silicon in TMAH solutions," *Sens. Actuators A*, vol. 34, no. 1, pp. 51–57, Jul. 1992.
- [32] N. F. Raley, Y. Sugiyama, and T. Van Duzer, "(100) silicon etch-rate dependence on boron concentration in ethylenediamine-pyrocatechol-water solutions," *J. Electrochem. Soc.*, vol. 131, no. 1, pp. 161–171, Jan. 1984.
- [33] U. Schnakenberg, W. Benecke, and P. Lange, "TMAHW etchants for silicon micromachining," in *Tech. Dig. 1991 Int. Conf. on Solid-State Sensors and Actuators (Transducers '91)*, San Francisco, 1989, pp. 815–818.
- [34] O. J. Glembocki, E. D. Palik, G. R. de Guel, and D. L. Kendall, "Hydration model for the molarity dependence of the etch rate of Si in aqueous alkali hydroxides," *J. Electrochem. Soc.*, vol. 138, no. 4, pp. 1055–1063, Apr. 1991.
- [35] H. Seidel, "The mechanism of anisotropic silicon etching and its relevance for micromachining," *Tech. Dig. 4th Int. Conf. on Solid-State Sensors and Actuators (Transducers '87)*, Japan, 1987, pp. 120–125. Also in R. S. Muller, et al., Eds., *Microsensors*. New York: IEEE Press, 1991, pp. 104–109.
- [36] Transene Co. Inc., "Material safety data sheet for aluminum etchant Type A," Transene Co., Inc., Rowley, MA, 1987.
- [37] D. J. Elliot, *Integrated Circuit Fabrication Technology, 2nd Ed.* New York: McGraw-Hill, 1989, p. 355.
- [38] J. E. A. M. van den Meerakker, M. Scholten, and J. J. van Oekel, "The etching of Ti-W in concentrated H<sub>2</sub>O<sub>2</sub> solutions," *Thin Solid Films*, vol. 208, no. 2, pp. 237–242, Feb. 1992.
- [39] M. G. Yang and K. M. Koliwad, "Auger electron spectroscopy of cleanup-related contamination on silicon surfaces," *J. Electrochem. Soc.*, vol. 122, no. 5, pp. 675–678, May 1975.
- [40] F. Pintchovski, J. B. Price, P. J. Tobin, J. Peavey, and K. Kobold, "Thermal characteristics of the H<sub>2</sub>SO<sub>4</sub>-H<sub>2</sub>O<sub>2</sub> silicon wafer cleaning solution," *J. Electrochem. Soc.*, vol. 126, no. 8, pp. 1428–1430, Aug. 1979.

- [41] W. Kern and D. A. Puotinen, "Cleaning solutions based on hydrogen peroxide for use in silicon semiconductor technology," *RCA Review*, vol. 30, no. 2, pp. 187-206, June 1970.
- [42] J. A. Amick, "Cleanliness and the cleaning of silicon wafers," *Solid State Technol.*, vol. 19, no. 11, pp. 47-52, Nov. 1976.
- [43] R. E. Dickerson, H. B. Gray, and G. P. Haight, Jr., *Chemical Principles*. Menlo Park, CA: Benjamin/Cummings, 1979.
- [44] O. J. Glembocki and E. D. Palik, "Hydration model for the molarity dependence of the etch rate of Si in aqueous alkali hydroxides," *J. Electrochem. Soc.*, vol. 138, no. 4, pp. 1055-63, Apr. 1991.
- [45] H. Nielsen and D. Hackleman, "Some illuminations on the mechanism of SiO<sub>2</sub> etching in HF solutions," *J. Electrochem. Soc.*, vol. 130, no. 3, pp. 708-712, Mar. 1983.
- [46] C. V. Macchioni, "The effect of substrate temperature and bias on the stress, chemical etch rate, and microstructure of high deposition rate sputtered SiO<sub>2</sub> films," *J. Vac. Sci. Technol. A*, vol. 9, no. 4, pp. 2302-2308, Jul./Aug. 1991.
- [47] P. Krulevitch, R. T. Howe, G. C. Johnson, and J. Huang, "Stress in undoped LPCVD polycrystalline silicon," in *Tech. Dig. 6th Int. Conf. on Solid-State Sensors (Transducers '91)*, San Francisco, CA, June 1991, pp. 949-952.
- [48] D. A. Jones, *Principles and Prevention of Corrosion*. New York: Macmillan, p. 290.
- [49] I. Stiharu, R. Bhat, M. Kahrizi, and L. Landsberger, "The influence of the stress state in silicon on the anisotropic etching process," *Proc. SPIE*, vol. 2015, (*Laser-Assisted Fabrication of Thin Films and Microstructures*), Quebec, Canada, pp. 254-262, Aug. 1993.
- [50] E. A. Irene, D. W. Dong, and R. J. Zeto, "Residual stress, chemical etch rate, refractive index, and density measurements on SiO<sub>2</sub> films prepared using high pressure oxygen," *J. Electrochem. Soc.*, vol. 127, no. 2, pp. 396-399, Feb. 1980.
- [51] S. M. Rossnagel, J. J. Cuomo, and W. D. Westwood, Eds., *Handbook of Plasma Processing Technology*. Park Ridge, NJ: Noyes, 1990.
- [52] M. A. Lieberman and A. J. Lichtenberg, *Principles of Plasma Discharges and Materials Processing*. New York: Wiley, 1994.
- [53] D. M. Manos and D. L. Flamm, Eds., *Plasma Etching: An Introduction*. Boston: Academic, 1989.
- [54] H. F. Winters and J. W. Coburn, "The etching of silicon with XeF<sub>2</sub>," *Appl. Phys. Lett.*, vol. 34, no. 1, pp. 70-73, Jan. 1979.
- [55] S. M. Sze, Ed. *VLSI Technology*. New York: McGraw Hill, 1983, chs. 2 and 8.
- [56] C. G. Keller and R. T. Howe, "Nickel-filled hexsil thermally actuated tweezers," in *Tech. Dig. 8th Int. Conf. on Solid-State Sensors and Actuators (Transducers '95)*, Stockholm, Sweden, June 1995, pp. 376-379.
- [57] H. Kinoshita and K. Jinno, "Anisotropic etching of silicon by gas plasma," *Japanese J. Appl. Phys.*, vol. 16, no. 2, pp. 381-382, Feb. 1977. *J. Electrochem. Soc.*, vol. 131, no. 9, pp. 161-171, Jan. 1984.
- [58] A. E. T. Kuiper and E. G. C. Lathouwers, "Room-temperature HF vapor-phase cleaning for low-pressure chemical vapor deposition of epitaxial Si and SiGe layers," *J. Electrochem. Soc.*, vol. 139, no. 9, pp. 2594-2599, Sept. 1992.
- [59] M. Wong, M. M. Moslehi, and R. A. Bowling, "Wafer temperature dependence of the vapor-phase HF oxide etch," *J. Electrochem. Soc.*, vol. 140, no. 1, pp. 205-208, Jan. 1993.
- [60] D. W. Oxtoby and N. H. Nachtrieb, *Principles of Chemistry*. Philadelphia: Saunders College Pub., 1986, p. 728.
- [61] D. E. Ibotson, D. L. Flamm, J. A. Mucha, and V. M. Donnelly, "Comparison of XeF<sub>2</sub> and F-atom reactions with Si and SiO<sub>2</sub>," *Appl. Phys. Lett.*, vol. 44, no. 12, pp. 1129-1131, June 1984.
- [62] E. Hoffman, B. Warneke, E. Kruglick, J. Weigold, and K. S. J. Pister, "3D Structures with piezoresistive sensors in standard CMOS," in *Proc. IEEE Micro Electro Mechanical Systems 1995*, Amsterdam, The Netherlands, Jan.-Feb. 1995, pp. 288-293.
- [63] W. Jost, *Diffusion in Solids, Liquids, Gases*. New York: Academic, 1952, chs. 10 and 11.
- [64] J. W. Coburn and H. F. Winters, "Plasma etching—A discussion of mechanisms," *J. Vac. Sci. Technol.*, vol. 16, no. 2, pp. 391-403, Mar.-Apr. 1979.
- [65] K. E. Petersen, "Silicon as a mechanical material," *Proc. IEEE*, vol. 70, no. 5, pp. 420-457, May 1982. Also in R. S. Muller, et al., Eds., *Microsensors*. New York: IEEE Press, 1991, pp. 39-76.
- [66] H. Guckel and D. W. Burns, "Fabrication techniques for integrated sensor microstructures," in *Tech. Dig. Int. Electron Devices Meet. 1986*, Los Angeles, CA, 1986, pp. 176-179.
- [67] M. Sekimoto, H. Yoshihara, and T. Ohkubo, "Silicon nitride single-layer x-ray mask," *J. Vac. Sci. Technol.*, vol. 21, no. 4, pp. 1017-1021, Nov./Dec. 1982.
- [68] C. H. Mastrangelo and R. S. Muller, "Vacuum-sealed silicon micro-machined incandescent light source," in *Tech. Dig. IEEE Int. Electron Devices Meet.*, Dec. 1989, pp. 503-506.
- [69] C. T.-C. Nguyen and R. T. Howe, "CMOS micromechanical resonator oscillator," in *Tech. Dig. IEEE Int. Electron Devices Meet.*, Dec. 1993, pp. 199-202.
- [70] K. R. Williams and R. S. Muller, "IC-processed hot-filament vacuum microdevices," in *Tech. Dig. IEEE Int. Electron Devices Meet.*, Dec. 1992, pp. 387-390.
- [71] K. E. Mattson, "Surface micromachined scanning mirrors," *Microelectron. Eng.*, vol. 19, pp. 199-204, 1992.



**Kirt R. Williams** (S'90) was born in Walnut Creek, CA, in 1964. He received the B.S. degree with high honors with a double major in electrical engineering and computer sciences (EECS) and materials science and engineering from the University of California, Berkeley, in 1987. He received the M.S. degree in EECS from UC-Berkeley in 1993.

While pursuing the B.S. degree, he worked at the Eastman Kodak Company and Altera Corporation, and after graduation he joined Western Digital Corporation working on digital and analog circuit design. He has been performing graduate work with the Berkeley Sensor & Actuator Center at UC-Berkeley since 1989. His main area of study is MEMS, with a thesis on micromachined hot-filament vacuum devices, for which he holds a patent. He has also been active in teaching and updating the department's IC-fabrication laboratory class.

Mr. Williams received the Electrical Engineering Outstanding Graduate Student Instructor Award from UC-Berkeley in 1996.



**Richard S. Muller** (M'62-SM'70-F'88-LF'96) received the degree of mechanical engineer from Stevens Institute of Technology, Hoboken, NJ, and the M.S.E.E. and Ph.D. degrees from the California Institute of Technology, Pasadena.

He joined the faculty in the Department of Electrical Engineering and Computer Science, University of California, Berkeley, in 1962, where he is now Professor in the Graduate School. He is a Co-Director and Co-Founder of the Berkeley Sensor and Actuator Center, an NSF/Industry/University

research center. He has been awarded NATO and Fulbright Research Fellowships.

Dr. Muller has been awarded the Alexander von Humboldt Senior Scientist Research Award winner, is a Member of the National Academy of Engineering, a Member of the Advisory Committee for the Electron Devices Society of IEEE, and a Trustee of the Stevens Institute of Technology. He serves on the IEEE Press Editorial Board and proposed, helped found, and is presently Editor-at-Large for the IEEE/ASME JOURNAL OF MICROELECTROMECHANICAL SYSTEMS (JMEMS). He has served as Chairman of the Steering Committee for the biennial Transducers Conference, as General Chairman of Transducers '91, and has chaired several technical committees for IEDM. Together with Dr. T. I. Kamins of Hewlett-Packard Co., he is the author of *Device Electronics for Integrated Circuits*, second edition (New York: Wiley, 1986). He is co-author of *Microsensors*, a volume in the IEEE Press Selected Reprint series published in 1990.